Journal of Metals, Materials and Minerals, 34(3), 2107, 2024

Phase separation promotes FCC-phase mechanical twinning in $AlCoCrFeMo_{0.05}Ni_2$ high entropy alloy

Zifeng ZHANG[1], Liang CHU[2], Jiqing ZHAO[3], Bing XU[1,*], and Qilu YE[1,*]

[1] *Anhui Engineering Research Center for High Efficiency Intelligent Photovoltaic Module, Chaohu University, Hefei, 238000, China*
[2] *School of Electronics and Information, Hangzhou Dianzi University, Hangzhou 310018, China*
[3] *Institute for Special Steels, China Iron and Steel Research Institute Group, Beijing 100081, China*

***Corresponding author e-mail**: 052059@chu.edu.cn, 052103@chu.edu.cn

Received date:
17 July 2024
Revised date:
29 July 2024
Accepted date:
6 August 2024

Keywords:
High entropy alloy;
Annealing;
Twin;
Deformation and fracture;
High-temperature

Abstract

The $AlCoCrFeMo_{0.05}Ni_2$ high entropy alloy (HEA) can remarkably enhance its ductility through high-temperature annealing. Nevertheless, the underlying mechanism remains under explored. Herein, we utilized molecular dynamics simulations (MD) to calculate the generalized stacking fault energy (GSFE) curves and uniaxial tensile behavior. Notably, the twin inclination of the FCC phase increases significantly after annealing. During plastic deformation, the FCC phase in the annealed alloy exhibits a substantially higher formation of twinning and stacking faults compared to the as-cast alloy. This increased twin inclination after annealing is the fundamental mechanism contributing to the enhancement of high-temperature ductility.

1. Introduction

The service temperature of nickel-based superalloys is limited by their melting point, currently around 1723 K [1]. With the continuous advancement of technology and the increasing demand for high-temperature materials in industry, there is an urgent need to develop new alloy materials capable of withstanding higher service temperatures to meet the requirements of aerospace, gas turbines, and other high-temperature applications. High-entropy alloys present themselves as a promising class of materials for high-temperature applications, surpassing traditional high-temperature alloys [2-6]. A prime example is the WNbMoTa alloy [4], which retains a remarkable strength of 400 MPa even at the elevated temperature of 1873 K. Despite this noteworthy strength retention, the alloy's compressive ductility is limited to only 2.0%. This trait is common among many high-strength high-entropy alloys, which tend to exhibit brittleness at room temperature and pose challenges in terms of castability. It is worth mentioning that testing protocols for these alloys often involve conditions that prioritize compression.

The $AlCoCrFeNi_{2.1}$ high-entropy alloy has garnered significant attention in recent years, mainly due to its remarkable castability [7-9]. First discovered by Lu *et al.* in 2014 [7], this alloy demonstrated a balanced strength-toughness combination at room temperature, albeit without exhibiting significant hardness advantages over traditional alloys. Current studies predominantly focus on enhancing its room-temperature properties, with limited exploration into improvements for high-temperature applications. For instance, Xiong *et al.* [8] introduced nano-precipitates into various phases of $AlCoCrFeNi_{2.1}$ through thermomechanical treatment, effectively increasing both its strength and toughness. Jiang *et al.* [9] utilized a combination of directional solidification and strong magnetic fields to control the microstructure and properties of eutectic high-entropy alloys, leveraging the alloy's tendency to form heterogeneous structures and short-range ordered phases to boost its room-temperature strength. To enhance the high-temperature strength of the $AlCoCrFeNi_{2.1}$ alloy, Mo was incorporated for the $AlCoCrFeMo_{0.05}Ni_2$ alloy [10-13]. This modification significantly improved the alloy's tensile strength at elevated temperatures. Upon annealing at 973 K for 150 h, the alloy exhibited an impressive elongation to failure of approximately 80% during tensile testing at 973 K [10]. This finding holds significant implications for the development of high-temperature alloys.

The primary microstructural change observed during annealing was the decomposition of the FCC phase [11-13]. Phase decomposition is a prevalent phenomenon in high-entropy alloys [14], which has been reported in various systems, such as CoCrFeNi [15], AlCrFeMnNi [16], and AlCoCrCuFeNi [17]. However, the mechanistic understanding of how phase decomposition impacts the high-temperature properties of alloys is still limited. The precise reasons for the remarkable enhancement in high-temperature ductility observed in the $AlCoCrFeMo_{0.05}Ni_2$ alloy due to phase decomposition have not been fully explained. This study aims to delve into the mechanical twinning behavior of the FCC phase both before and after annealing, with the objective of elucidating the factors that contribute to the observed increase in high-temperature plasticity following annealing.

2. Experimental

Thermo-Calc software and the TChigh-entropy alloy4.2 database were utilized for composition calculations, which have been reliably validated in numerous researches [18-20]. The composition of the as-cast alloy was determined using the Sheil solidification model. For the annealed alloy, equilibrium phase diagrams were employed. The LAMMPS software was utilized for both the calculation of the GSFE and the uniaxial tensile behavior [21]. A mixed potential energy function was utilized by combining the embedded atom method (EAM) potential function for AlCoCrFeNi [22] and the Finnis-Sinclair (FS) potential function for Mo [23]. The accuracy of calculating generalized stacking fault energy using LAMMPS primarily depends on the choice of potential function. The potential function used in this paper has been validated in multiple aspects, such as lattice constants, stacking fault energy, and elastic constants [22,23], confirming its reliability in stacking fault energy calculations. For visual analysis purposes, the OVITO software [24] was utilized. The atoms were subjected to neighbor analysis (CNA). The dislocations induced by tensile deformation were analyzed using the dislocation analysis (DXA) method.

The calculation of the GSFE was conducted under 0 K. The simulation cell was a 10 × 10 × 40 supercell. The x-, y-, and z-axes were oriented along the [112], [-110], and [-1-11] directions, respectively. Periodic boundary conditions were applied along the x- and y-axes, while free boundary conditions were adopted for the z-axis. For the uniaxial tensile simulation, a 20 × 60 × 20 simulation cell was employed. Periodic boundary conditions were implemented along the x- and z-axes. The model underwent energy minimization using the conjugate gradient algorithm. Subsequently, a relaxation simulation using the NPT ensemble was conducted for 50 ps at a temperature of 973 K. After equilibration, a uniaxial tensile test is performed on the model using the deform command along the y-direction with a strain rate of 1×10^9 s^{-1}. During the tensile process, stress and strain data are recorded, and the simulation trajectory is saved. Subsequently, the stress-strain curve obtained from the tensile simulation is analyzed to extract important mechanical properties of the material, such as yield strength and tensile strength. Additionally, by analyzing the simulation trajectory, the deformation behavior of the material during tensile testing, such as plastic deformation, strain hardening, and ultimate fracture, can be observed.

The alloy was prepared by arc melting with a weight of 5 kg. For microstructure analysis, transmission electron microscopy (TEM) samples were prepared using a twin-jet polisher at 258 K with a 6% perchloric acid alcohol solution for electrolytic polishing. To simulate the heat treatment state of the alloy at high temperatures, annealing was performed in a box-type resistance furnace. Before annealing, the furnace was calibrated using a thermometer to ensure accurate temperature control. The annealing temperature was set to 973 K and the duration was 48 h, with air as the annealing medium.

3. Results and discussion

The microstructural evolution of the $AlCoCrFeMo_{0.05}Ni_2$ high-entropy alloy following annealing at 973 K for 48 h was investigated using transmission electron microscopy (TEM), as shown in Figure 1. TEM analysis revealed significant microstructural changes, showcasing the impact of thermal treatment on the stability of this high-entropy alloy system. As shown in Figure 1(a-c), the initial FCC solid solution phase underwent decomposition, leading to the formation of a (Ni, Al)-rich phase. This phase decomposition likely results from the thermodynamic driving force for the system to minimize its free energy, seeking a more stable configuration at elevated temperatures. Further investigation into the deformation mechanisms operating at elevated temperatures was carried out through TEM analysis of the fracture surface after high-temperature tensile testing at 973 K. Figure 1(d) clearly demonstrates the presence of deformation twinning near the fracture surface, indicating that this mechanism plays a crucial role in accommodating plastic deformation at elevated temperatures. The occurrence of deformation twinning is likely a contributing factor to the observed enhancement in high-temperature ductility, as it provides an alternative mechanism for slip and strain accommodation, thereby delaying the onset of fracture.

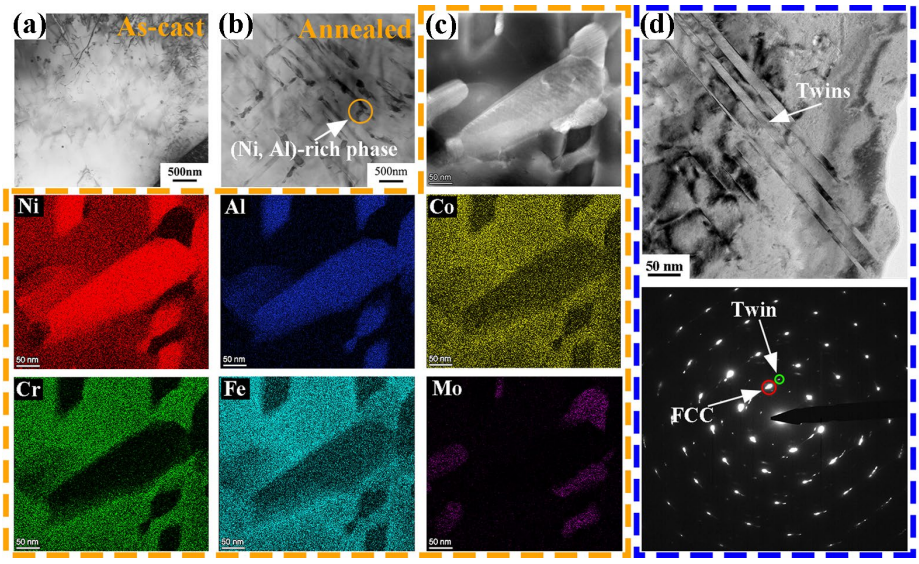

Figure 1. Phase separation and mechanical twins of $AlCoCrFeMo_{0.05}Ni_2$ HEA: (a) As-cast alloy, (b) Annealed alloy, (c) EDS result of (Ni, Al)-rich phase, and (d) Mechanical twins.

The compositional analysis of the AlCoCrFeMo$_{0.05}$Ni$_2$ high-entropy alloy was conducted using a combination of phase diagram calculations and experimental techniques. The results of the phase diagram calculations, displayed in Figure 2 and summarized in Table 1, provide a detailed understanding of the equilibrium phases present in the alloy. Furthermore, energy spectrum analysis of the FCC phase in the as-cast alloy exhibited excellent agreement with the calculated results, confirming the reliability of the computational methodology. Despite the inherent limitations of current energy spectrum measurement techniques, particularly with regards to potential measurement errors, the calculated compositions will serve as valuable input parameters for subsequent studies.

A comparison of the FCC phase composition in the as-cast alloy with that of the annealed alloy reveals significant compositional shifts. Notably, the Ni and Co contents exhibited a substantial increase following annealing, while the Al and Mo contents displayed a notable decrease. The remaining elements demonstrated minimal compositional changes. These observations suggest that the annealing process induces a redistribution of elements within the FCC phase, leading to a preferential enrichment of Ni and Co and a depletion of Al and Mo. This compositional redistribution likely plays a significant role in the microstructural evolution observed in the annealed alloy, contributing to the formation of the (Ni, Al)-rich phase and potentially influencing the alloy's mechanical behavior at elevated temperatures. Further investigation into the driving forces behind this compositional redistribution, as well as its impact on the alloy's properties, is warranted.

To elucidate the influence of annealing on the stacking fault energies (SFEs) in the AlCoCrFeMo$_{0.05}$Ni$_2$ high-entropy alloy, we employed large-scale atomistic simulations. The calculated generalized stacking fault energy curves are presented in Figure 3. Figure 3(a) depicts the FCC simulation cell of the AlCoCrFeMo$_{0.05}$Ni$_2$ high-entropy alloy, showcasing the atomic arrangement within the unit cell.

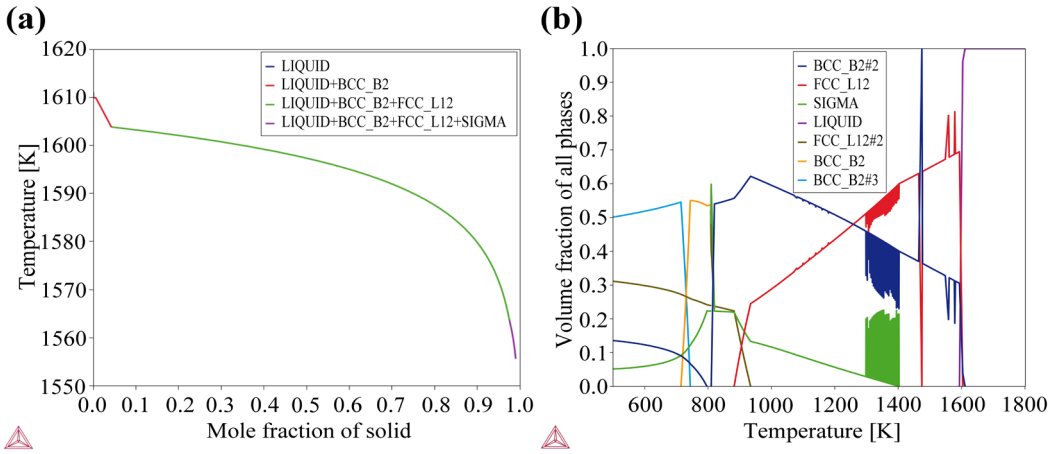

Figure 2. Phase diagram of AlCoCrFeMo$_{0.05}$Ni$_2$ HEA: (a) Sheil model, and (b) Equilibrium phase diagram.

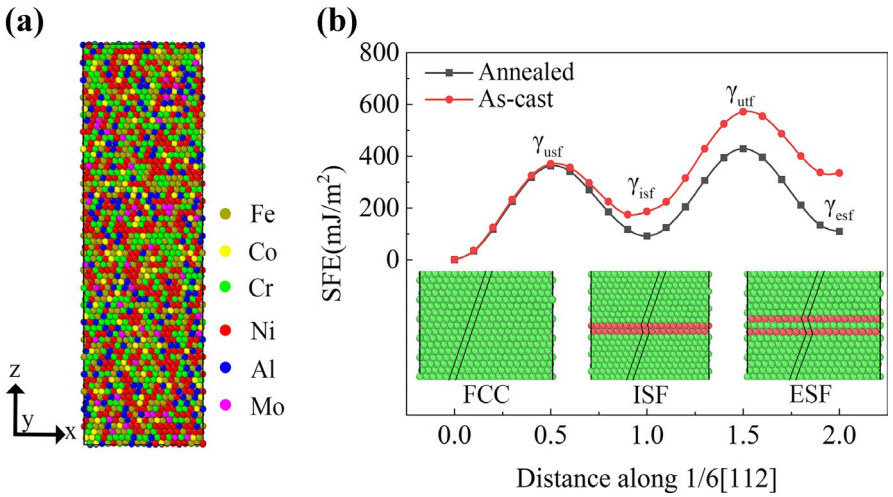

Figure 3. Generalized Stacking Fault Energy Curves of AlCoCrFeMo$_{0.05}$Ni$_2$ HEA.

Table 1. Compositions of the FCC phase in AlCoCrFeMo$_{0.05}$Ni$_2$ HEA (at.%).

Ni	Al	Co	Cr	Fe	Mo	State
34.05	10.75	8.33	23.85	20.22	2.80	As-cast
41.88	3.89	12.54	21.13	20.49	0.07	Annealed

The GSFE curves in Figure 3(b) provide valuable insights into the stability of different stacking fault configurations. The first peak in each curve corresponds to the unstable stacking fault energy (γ_{usf}), while the first valley represents the intrinsic stacking fault energy (γ_{isf}). The second peak indicates the unstable twin nucleation energy (γ_{utf}), and the second valley corresponds to the extrinsic stacking fault energy (γ_{esf}). These energies represent the energetic barriers associated with the formation and propagation of different types of stacking faults, influencing the plastic deformation behavior of the material.

Comparing the calculated SFE values for the as-cast and annealed alloys reveals significant differences. The as-cast alloy exhibits a γ_{utf} of 571.6 mJ·m^{-2}, a γ_{usf} of 370.3 mJ·m^{-2}, and a γ_{isf} of 186.3 mJ·m^{-2}. In contrast, the annealed alloy displays lower values: γ_{utf} = 429.1 mJ·m^{-2}, γ_{usf} = 362.7 mJ·m^{-2}, and γ_{isf} = 91.7 mJ·m^{-2}. This reduction in SFE values, particularly for γ_{isf} and γ_{utf}, suggests that the annealing process enhances the propensity for twinning and stacking fault formation in the alloy. This change in SFE behavior is likely attributed to the compositional redistribution and microstructural evolution observed during annealing, highlighting the strong correlation between composition, microstructure, and mechanical properties in this high-entropy alloy system.

Swygenhoven *et al.* [25] and Siegel *et al.* [26] suggested that the twinning propensity of FCC metals can be determined by the difference in energy barriers between nucleating a leading Shockley dislocation on an adjacent slip plane and nucleating a trailing dislocation on the original slip plane. The twinning propensity of FCC metals can be expressed as,

$$\delta = (\gamma_{utf} - \gamma_{isf}) - (\gamma_{usf} - \gamma_{isf}) = \gamma_{utf} - \gamma_{usf} \quad (1)$$

After calculation, the as-cast alloy had a δ value of 201.3 mJ·m^{-2}, while the annealed alloy had a δ value of 66.4 mJ·m^{-2}. A smaller δ value indicates a higher propensity for twinning. Therefore, the annealed twinning exhibits a stronger twinning propensity.

Tadmor *et al.* [27,28] proposed a theoretical model of dislocation nucleation from the crack tip. They statistically averaged the Schmid factors for various orientations of polycrystalline metals and expressed them as functions of γ_{isf}, γ_{usf}, and γ_{utf}, where,

$$\tau_a = \frac{K_\perp}{K^T} = \left[1.136 - 0.151\,\frac{\gamma_{isf}}{\gamma_{usf}}\right]\sqrt{\frac{\gamma_{usf}}{\gamma_{utf}}} \quad (2)$$

The calculated values of τ_a for the as-cast and annealed alloy are 0.6478 and 0.8453, respectively. A higher τ_a value indicates a stronger twinning propensity in FCC metals. Thus, the annealed alloy demonstrates a higher propensity for twinning and a greater likelihood of twinning nucleation.

Cai *et al.* [29] proposed an expression for the intrinsic twinning propensity of FCC metals, which is based on the homogeneous nucleation mechanism of Shockley dislocations. The expression is as follows,

$$\eta = \frac{\tau_{max}^{[\bar{1}2\bar{1}]}}{\tau_{max}^{[\bar{2}11]}} = \frac{\gamma_{usf} - \gamma_{isf}}{\gamma_{utf} - \gamma_{isf}} \quad (3)$$

The calculated values of η for the as-cast and annealed alloy are 0.4775 and 0.8032, respectively. A higher value of η suggests a greater propensity for twinning and plastic deformation in FCC metals. Thus, the annealed alloy demonstrates a higher propensity for twinning and plastic deformation.

Figure 4 illustrates the results of uniaxial tensile simulation on $AlCoCrFeMo_{0.05}Ni_2$ HEA. The stress-strain curves in Figure 4(a) shows both the as-cast and annealed alloy undergoing an elastic phase followed by a plastic phase. In the elastic phase, the annealed alloy demonstrates a slightly higher elastic modulus compared to the as-cast alloy. However, the elastic limit (i.e., stiffness) of the annealed alloy is much higher than that of the as-cast alloy. The focus of this study primarily lies in the plastic phase of tensile deformation. In the general yield stage, there is a noticeable yield drop and yield plateau. One can see that both cases exhibit fluctuating yield plateaus, indicating significant microstructural changes during the tensile process.

To analyze the plastic deformation capability of the as-cast and annealed alloy, the stress drop's lowest points are analyzed (Figure 4(c-d)). The annealed alloy predominantly undergoes twinning, while the as-cast alloy primarily experiences intrinsic and extrinsic stacking faults. Both twinning and stacking faults contribute to plastic deformation, but deformation twinning generally exhibits higher plastic deformation capability [30].

In Figure 4(b), one can see that the amount of HCP phase formed during plastic deformation is significantly higher in the annealed alloy compared to the as-cast, indicating a higher presence of twinning and stacking faults in the annealed alloy. This suggests that the annealed alloy has more pathways for stress release during plastic deformation, resulting in a higher plastic deformation capability. From the DXA results of points e and f (Figure 4(e-f)), one can see that twinning remains relatively stable in the annealed alloy. Furthermore, additional intrinsic stacking faults are formed between twin boundaries, which further release deformation stress and enhance plastic deformation. In contrast, the as-cast alloy primarily consists of intrinsic and extrinsic stacking faults, which promote plastic deformation only through annihilation and new formation. Therefore, the increasing of tendency for twinning in the FCC phase through annealing is one of the main factors contributing to the improvement of high-temperature plasticity in the $AlCoCrFeMo_{0.05}Ni_2$ HEA.

The exploration of high-temperature plasticity in high-entropy alloys holds immense promise for overcoming their inherent brittleness and unlocking new frontiers in material design. This research area offers compelling pathways to enhance HEA performance, addressing critical challenges in high-temperature applications. One primary avenue for improvement lies in mitigating the brittleness often associated with high-performance HEAs. By harnessing the enhanced plasticity observed at elevated temperatures, researchers can significantly improve ductility, thereby enhancing reliability and robustness in demanding applications subjected to high stress and strain. Furthermore, the high-temperature plasticity of HEAs presents an unprecedented opportunity to engineer materials with exceptional strength-ductility combinations. This opens up a new paradigm for developing novel HEAs that possess both high strength and excellent formability, making them ideal candidates for demanding engineering applications where both mechanical properties are crucial.

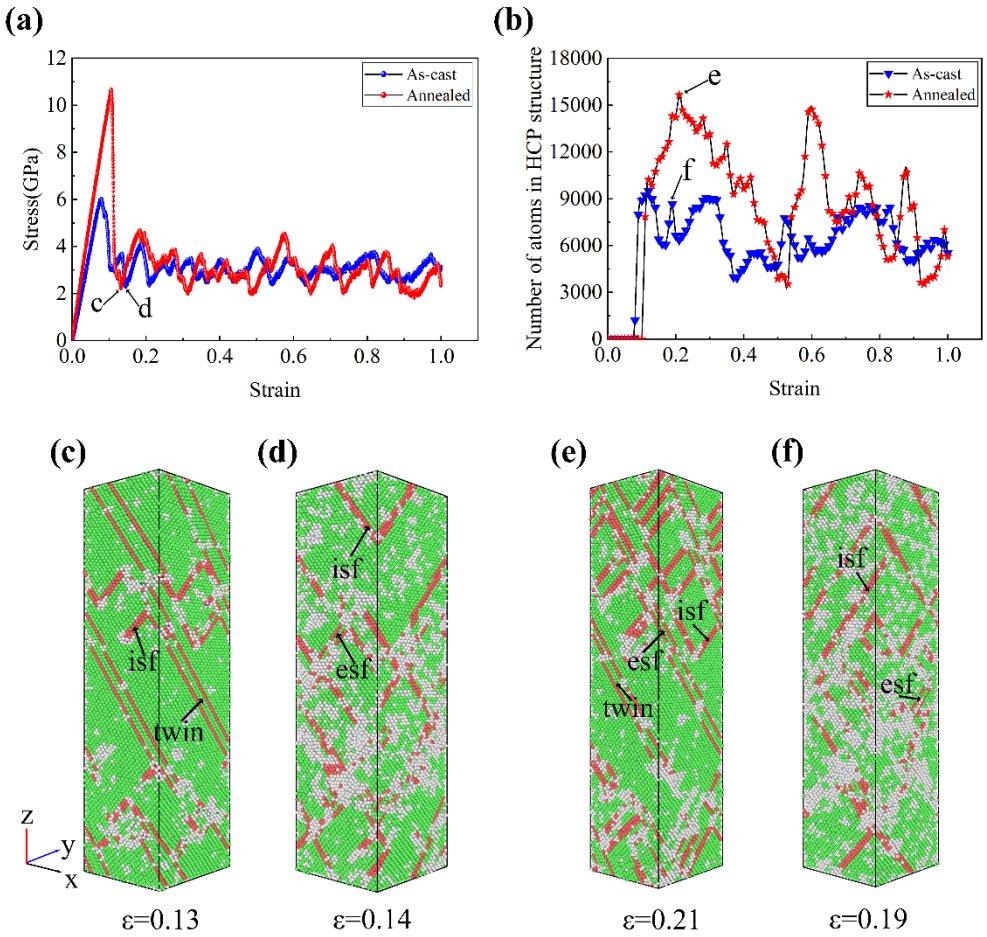

Figure 4. Uniaxial tensile simulation on $AlCoCrFeMo_{0.05}Ni_2$ HEA: (a) Stress-strain curves, (b) The amount of HCP phase, (c, d) DXA results of points c and d, (e, f) DXA results of points e and f.

The potential applications of high-temperature plasticity in HEAs highlight the immense relevance and promise of this research field for the advancement of high-temperature alloys. By meticulously tailoring microstructures and enhancing properties through innovative material design, researchers can revolutionize the design and performance of advanced materials for a wide range of high-temperature applications, paving the way for significant breakthroughs in various industries.

4. Conclusions

(1) $AlCoCrFeMo_{0.05}Ni_2$ alloy experienced the decomposition of the FCC solid solution phase into a (Ni,Al)-rich phase during annealing, leading to significant changes in both structure and performance.

(2) The calculated GSFE curve provided insights into the mechanical properties of the alloy. Evaluation of δ and τa values indicated a higher propensity for twinning in the annealed alloy, confirming its increased likelihood of twin nucleation. The η values also demonstrated a greater tendency for twinning and plastic deformation in the annealed alloy, highlighting its improved plasticity under high-temperature conditions.

(3) The annealed alloy displayed superior performance, primarily driven by deformation twinning and slip stacking mechanisms. Presence of a larger amount of HCP phase during plastic deformation in the annealed alloy indicated more pronounced twinning and stacking fault activity, contributing to its enhanced plastic deformation capability.

Acknowledgment

This work was supported by the University Natural Science Research Project of Anhui Province (CN) [2022AH051721], the Natural Science Foundation of Anhui Province (CN) [2308085ME138], the Starting Research Fund from Chaohu University (KYQD-2023023), and the Development of an Artificial Intelligence-Based Wide Wind Speed Vector Detection and Wind Energy Collection System [hxkt20230068].

References

[1] R. Darolia, "Development of strong, oxidation and corrosion resistant nickel-based superalloys: critical review of challenges, progress and prospects," *International Materials Reviews*, vol. 64, pp. 355-380, 2018.

[2] B. Cantor, "Multicomponent and high entropy alloys," *Entropy*, vol. 16, pp. 4749-4768, 2014.

[3] Y. Hu, and Y. Liu, "Constitutive behavior of semi-solid $Al_{80}Mg_5Li_5Zn_5Cu_5$ light-weight high entropy alloy," *Journal of Materials Research and Technology*, vol. 29, pp. 5713-5720, 2024.

[4] O. N. Senkov, G. B. Wilks, D. B. Miracle, C. P. Chuang, and P. K. Liaw, "Refractory high-entropy alloys," *Intermetallics*, vol. 18, pp. 1758-1765, 2010.

[5] X. Feng, Y. Yue, J. Qiu, J. Qiu, H. Jain, and S. Zhou, "Entropy engineering in inorganic non-metallic glass," *Fundamental Research*, vol. 2, pp. 783-793, 2022.

[6] M. Ma, X. Yang, H. Meng, Z. Zhao, J. He, and Y. Chu, "Nanocrystalline high-entropy hexaboride ceramics enable remarkable performance as thermionic emission cathodes," *Fundamental Research*, vol. 3, pp. 979-987, 2023.

[7] Y. Lu, Y. Dong, S. Guo, L. Jiang, H. Kang, T. Wang, B. Wen, W. Zhijun, J. C. Jie, Z. Cao, H. H. Ruan, and Y. Lu., "A promising new class of high-temperature alloys: eutectic high-entropy alloys," *Scientific reports*, vol. 4, p. 6200, 2014.

[8] T. Xiong, S. Zheng, J. Pang, and X. Ma, "High-strength and high-ductility $AlCoCrFeNi_{2.1}$ eutectic high-entropy alloy achieved via precipitation strengthening in a heterogeneous structure," *Scripta Materialia*, vol. 186, pp. 336-340, 2020.

[9] X. Jiang, Y. Li, P. Shi, Y. Yang, M. Wang, J. Huang, Y. Qin, Y. Lin, B. Tan, Y. Ruan, X. Wang, B. Zhou, B. Ding, Q. Li, Z. Shen, T. Zheng, C. Liu, P. K. Liaw, and Y. Zhong, "Synergistic control of microstructures and properties in eutectic high-entropy alloys via directional solidification and strong magnetic field," *Journal of Materials Research and Technology*, vol. 28, pp. 4440-4462, 2024.

[10] Q. Ye, G. Yang, and B. Yang, "Effect of aging on microstructure and property of $AlCoCrFeMo_{0.05}Ni_2$ high entropy alloy," *Materials Science and Engineering: A*, vol. 760, pp. 1-6, 2019.

[11] Q. Ye, G. Yang, and B. Yang, "Segregation engineering in a promising heat-resistant $AlCoCrFeMo_{0.05}Ni_2$ high entropy alloy," *Journal of Alloys and Compounds*, vol. 869, p. 159336, 2021.

[12] Q. Ye, B. Yang, G. Yang, J. Zhao, and Z. Gong, "Stability prediction of $AlCoCrFeMo_{0.05}Ni_2$ high entropy alloy by Kinetic Monte Carlo method," *Materials Letters*, vol. 306, p. 130907, 2022.

[13] Q. Ye, Z. Zhang, Q. Wang, X. Xu, K. Wang, J. Zhao, B. Xu, J. Zhang, D. Liu, Y. Deng, X. Qian, Q. Wu, Y. Wang, Q. Cao, "Promoting nanoscale deformation twinning through FCC phase decomposition in $AlCoCrFeMo_{0.05}Ni_2$ high entropy alloy," *Journal of Alloys and Compounds*, vol. 985, p. 174086, 2024.

[14] H. Luan, L. Huang, J. Kang, B. Luo, X. Yang, L. Jinfeng, Z. Han, J. Si, Y. Shao, J. Lu, and K. Yao, "Spinodal decomposition and the pseudo-binary decomposition in high-entropy alloys," *Acta Materialia*, vol. 248, p. 118775, 2023.

[15] F. He, Z. Wang, Q. Wu, J. Li, J. Wang, and C. T. Liu, "Phase separation of metastable CoCrFeNi high entropy alloy at intermediate temperatures," *Scripta Materialia*, vol. 126, pp. 15-19, 2017.

[16] A. Munitz, L. Meshi, and M. J. Kaufman, "Heat treatments' effects on the microstructure and mechanical properties of an equiatomic Al-Cr-Fe-Mn-Ni high entropy alloy," *Materials Science and Engineering: A*, vol. 689, pp. 384-394, 2017.

[17] S. Singh, N. Wanderka, B. S. Murty, U. Glatzel, and J. Banhart, "Decomposition in multi-component AlCoCrCuFeNi high-entropy alloy," *Acta Materialia*, vol. 59, pp. 182-190, 2011.

[18] S. R. Oke, O. E. Falodun, A. Bayode, U. Anamu, and P. Olubambi, "Phase prediction, densification, and microstructure of AlCrFeNi $(TiO_2)_x$ high entropy alloy composite fabricated by spark plasma sintering," *Journal of Alloys and Compounds*, vol. 968, p. 172030, 2023.

[19] A. Bansal, P. Kumar, S. Yadav, V. Hariharan, M. Rahul, and G. Phanikumar, "Accelerated design of high entropy alloys by integrating high throughput calculation and machine learning," *Journal of Alloys and Compounds*, vol. 960, p. 170543, 2023.

[20] S. Güler, E. D. Alkan, and M. Alkan, "Vacuum arc melted and heat treated $AlCoCrFeNiTi_X$ based high-entropy alloys: Thermodynamic and microstructural investigations," *Journal of Alloys and Compounds*, vol. 903, p. 163901, 2022.

[21] P. Steve, "Fast parallel algorithms for short-range molecular dynamics," *Journal of computational physics*, vol. 117, pp. 1-19, 1995.

[22] F. Diana, and A. Caro, "Model interatomic potentials for Fe–Ni–Cr–Co–Al high-entropy alloys," *Journal of Materials Research*, vol. 35, pp. 3031-3040, 2020.

[23] G. Ackland, and R. Thetford, "An improved N-body semi-empirical model for body-centred cubic transition metals," *Philosophical Magazine A*, vol. 56, pp. 15-30, 1987.

[24] S. Alexander, "Visualization and analysis of atomistic simulation data with OVITO–the Open Visualization Tool," *Modelling and simulation in materials science and engineering*, vol. 18, p. 015012, 2009.

[25] H. Swygenhoven, P. Derlet, and A. Frøseth, "Stacking fault energies and slip in nanocrystalline metals," *Nature materials*, vol. 3, pp. 399-403, 2004.

[26] D. Siegel, "Generalized stacking fault energies, ductilities, and twinnabilities of Ni and selected Ni alloys," *Applied Physics Letters*, vol. 87, p. 121910, 2005.

[27] E. Tadmor, and N. Bernstein, "A first-principles measure for the twinnability of FCC metals," *Journal of the Mechanics and Physics of Solids*, vol. 52, pp. 2507-2519, 2004.

[28] N. Bernstein, and E. Tadmor, "Tight-binding calculations of stacking energies and twinnability in FCC metals," *Physical Review B*, vol. 69, p. 094116, 2004.

[29] T. Cai, Z. Zhang, P. Zhang, J. Yang, and Z. Zhang, "Competition between slip and twinning in face-centered cubic metals," *Journal of Applied Physics*, vol. 116, p. 163512, 2014.

[30] J. Kim, M. Kwon, and B. C. De Cooman, "On the deformation twinning mechanisms in twinning-induced plasticity steel," *Acta Materialia*, vol. 141, pp. 444-455, 2017.